The Ash Deposition Mechanism in Boilers Burning Zhundong Coal with High Contents of Sodium and Calcium: a Study from Ash Evaporating to Condensing

Xuebin Wang[a,], Bo Wei[a], Yibin Wang[a], Tao Yang[a], Houzhang Tan[a],Hrvoje Mikulčić[b],Milan Vujanović[b], Neven Duić[b]*

[a] MOE Key Laboratory of Thermo-Fluid Science and Engineering, Xi'an Jiaotong University, Xi'an 710049, China

[b] Faculty of Mechanical Engineering and Naval Architecture, University of Zagreb, Ivana Lučića 5, 10000 Zagreb, Croatia

*Corresponding Author. E-mail: wxb005@mail.xjtu.edu.cn, tel/fax: +86-029-82668703

ABSTRACT:

The high contents of sodium and calcium in Zhundong coal induce severe slagging and ash deposition in boilers. In this study, the ash deposition mechanism was investigated based on the results obtained from a full-scale boiler (350 MW) burning Zhundong coal, anda fixed bed reactor used for ash evaporating-condensing. In the full-scale boiler, the condensing and depositing of sodium and calcium sulfates play an important role on ash depositing on convection heating surfaces. Sulfates start to significantly condense and deposit at the flue gas temperature of about 850 °C (at Medium and High Temperature Reheater). Ash evaporating tests proved that, with the increasing in temperature from 400 °C to 1200 °C, the ash evaporating process is divided into three stages: 1) 400-800 °C, 80% of sodium, and 100% of chlorine are released; 2) 800-1000 °C, all the left sodium evaporates and sulfur starts to be released with the formation of partial aluminosilicates; 3) 1000-1200 °C, all the left sulfur is released through the decomposition of calcium sulfates and then calcium starts to evaporate, while silicon oxides disappears due to the formation of new complex silicates. Ash condensing tests further proved that, the sodium in Zhundong coal was released mainly in the forms of atom, oxide, and chloride, in which sodium chloride account for about 50%. When the evaporating temperature increased higher than 1000 °C, partial alkali and alkaline earth metals were released as gaseous sulfates, and afterwards condense and deposit on the heating surfaces. At last, a temperature-dependent ash deposition mechanism in Zhundong coal combustion was proposed.

KEYWORDS:

Zhundong Coal; Ash deposition; Sodium; Calcium; Sulfur.

Introduction

Zhundong, located in the east of Junggar Basin, Xinjiang, China, with the forecast reserves of 390 billion tons is the largest intact coalfield in the world. According to the current coal consumption in China, the Zhundong coal could meet the needs for coal consumption in China for the next 100 year [1, 2]. Zhundong coal is characterized by high ignition quality and low environmental threat due to the high volatile content and ultralow ash and sulfur contents. However, similar with the brown coal in Australia [3-6], the content of sodium in Zhundong coal ash is very high, generally more than 5%, far more than the normal sodium content level in typical Chinese coal, usually between 1 and 2 % [7, 8]. Consequently severe problems of slagging, fouling, and corrosion on boiler heating surfaces are induced, which deteriorate the heat flux, efficiency, and lifetime of a boiler [9]. Xi'an Thermal Power Research Institue (TPRI) investigated the slagging and fouling status quo of dozens of boilers burning Zhundong coal in Xinjiang, China. It indicated that boilers would be under great threat from slagging when the sodium content in coal ash exceeded 2.5 and 3 % for 100MW and 225-350 MW boilers, respectively. The boiler adaptability of even larger capacity 600-1000 MW on high sodium coal is still unknown [7].

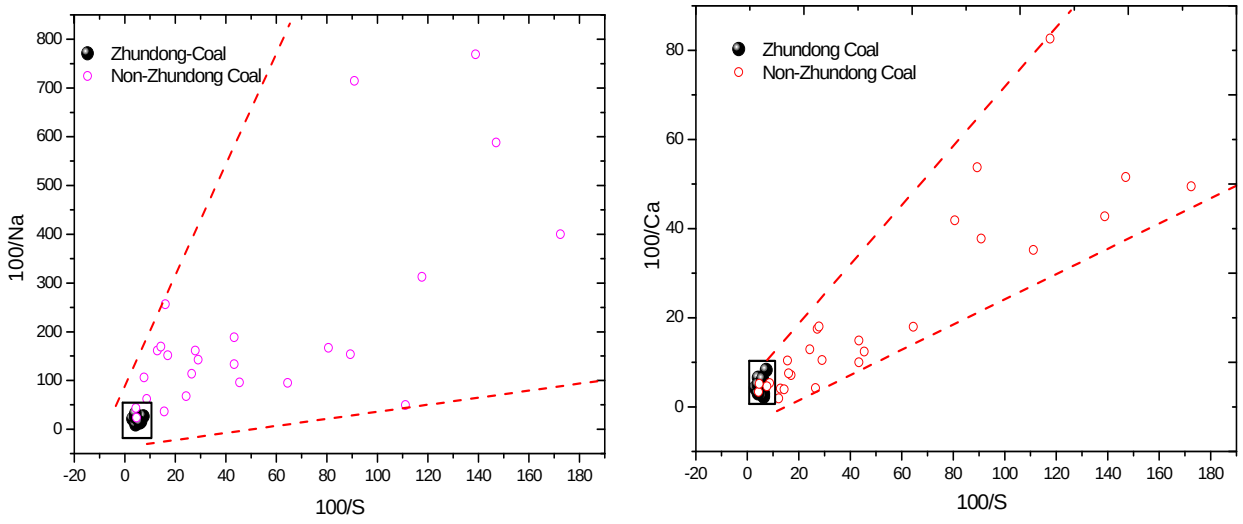

(a) 100/Na vs 100/S *(b) 100/Ca vs 100/S*

Figure 1. The contents of Na, Ca and S in Xinjiang Zhundong Coal ash and Non-Zhundong Coal ash (eight kinds of Zhundong Coal and twenty-seven kinds of Non-Zhundong Coal, and e.g. 100/Na refering to the inverse of Na content in ash)

In this study eight kinds of Zhundong coal were compared with twenty-seven kinds of non-Zhundong coal very commonly used in China, including bituminous, sub-bituminous, and lignite coal. The inverse values of sodium, calcium and sulfur content in ash are plotted in Figure 1, showing that Zhudnong coal is astricted to a very limited region. It can also be observed that the calcium and sulfur contents in Zhundong coal ash were much higher than the average contents in non-Zhundong coal ash. The contents of calcium and sulfur in certain types of Zhundong coal ash are higher than 30 %, and in some cases even 40 %. Harbin Boiler Company has conducted a test in a 300 MW boiler co-firing Zhundong coal, and after a dozen days operation, the convection heating surfaces were blocked by severe slagging and ash deposition. In this test, a high amount of calcium sulfates was found in the slags and deposits [10]. These observations indicated that beside sodium, calcium and sulfur species also play an important role in the slagging and ash depositing process.

Recently, only a few studies investigated the Zhundong coal slagging. He et al. [11] used Laser-Induced Breakdown Spectroscopy (LIBS) to measure atomic sodium emissions in Zhundong coal combustion under low O_2 concentration (3.9-10.6 %, oxygen-fuel combustion). The study showed that very little sodium was released from the Zhundong coal's volatile matters, 20-38 % was released from the char content , and 60-78 % was released from the ash content.. The study also showed that the ratio of potassium released from the char content was enhanced by O_2 but inhibited by CO_2 concentration. Zhou et al. [12, 13] developed an ash deposition probe with CCD and heat flux monitoring system to on-line record the deposition thickness and heat flux in a 300KW test furnace. It was found that the deposit growth process was composed of four stages and that the slagging deposits showed layer structures, however the enrichment of alkali and alkali-earth metal was not found in each deposition layer. Xu et al. [1] compared the ash properties from Zhundong coal co-firing in a lab-scale drop tube furnace and a power plant boiler, which agreed well. The study showed that particles smaller than 10 μm had higher Ca, Fe, and Mg content, while the weight fractions of sodium and potassium were not that high. In another study on Zhundong coal slagging, the ash deposits were collected from different positions in a 30 MW subcritical boiler. The chemical analysis showed that the ash fouling on the superheater tubes was formed with a thinner Fe-rich layer followed by the deposition of Na_2SO_4 liquids. The slagging in the water cooled wall was mainly induced by the low-temperature eutectics from the interaction of CaO and Fe_2O_3 on the receding char surface, and the eutectic Ca-Al-Si containing Fe^{2+}-bearing oxide [9]. The other studies on Zhundong coal slagging were mainly focused on the ash fusion and melting by using lab-scale furnaces and ash melting apparatus.

Meng [14] found that the low-temperature eutectics of ferrum and aluminosilicate played an important role in the high-temperature sintering of Zhundong coal ash and its slagging near the water cooled wall. It was also found that this phenomena is comparatively affected by O_2 concentration. Wang et al. [15] following the State Standard of GB/T 212-2008 and GB/T 219-1996, measured the ash melting temperature for different Zhundong coal co-firing tests. The study showed that there was a worst co-firing ratio for the lowest melting temperature. However, the most recent work [16] pointed out that the two named Standards were not suitable for the evaluation of Zhundong coal ash melting, since the softening temperature decreased by 100^{o}C, when the ashing temperature was lowered from 815 to 500 ^{o}C.

Summarizing the previous results, the authors note that the slagging problem in Zhundong coal combustion is mainly ascribed to two reasons: (1) the formation of low-temperature eutectics containing ferrum at high furnace temperatures in the water cooled wall region, and (2) re-condensing of evaporated alkali and alkaline earth metals (AAEMs) at lowered gas temperatures in the convection heating surface region. The melting or fusion of eutectics containing ferrum has been widely reported, regardless of coal types, and it mainly depends upon the primary components in coal ash like silicon, aluminum, and calcium. However, the transformation of AAEMs is more associated to coal types, for Zhundong coal as newly found low-rank lignite with extremely high sodium and calcium content, the understanding of AAEMs transformation and ash deposition is still insufficient.

Therefore, this study aims to demonstrate ash deposition mechanism in the convection heating surface region of boilers burning Zhundong coal, via incorporating the tests in a full-scale boiler and in a lab-scale fixed bed reactor. In the full-scale 350 MW boiler, the slags and deposits were collected and analyzed at different convection heating surfaces along the gas flow direction. Moreover, a special temperature-controlled condensing probe, above the fuel stack, was designed to capture the released AAEMs vapor in a fixed bed reactor. The residual solid ash and the captured condensed species were analyzed by using X-ray fluorescence (XRF), X-ray diffraction (XRD), scanning electron microscope (SEM), and energy dispersive spectrometer (EDS). The research goal is to build a full transformation mechanism of sodium and calcium from the Zhundong coal, through evaporating and condensing, to deposits in boilers.

1. Experimental Section

2.1 Fuel Properties

Since there are no boilers that could compleately be operated on Zhundong coal , in the full-scale test Zhundong (ZD) coal was co-fired with Zhunnan (ZN) coal, while in lab-scale test only ZD coal was used. The fuel properties of ZD

and ZN coal are compared in Table 1. The water content in ZD coal is twice of that in ZN coal, while the ash content in ZD coal is lower than in the ZN coal. Note that the ash fusion temperatures (DT, ST, and HT) of ZD coal are higher than that of ZN coal by 120 ^{o}C, even if the slagging of ZD coal is much more severe. The contents of calcium and sodium in ZD coal ash are over 40 % and 6 %, respectively. These two contents are much higher in ZD coal than that in ZN coal, however the ferrum content in ZD and ZN coal ash is almost the same. The comparison of fuel properties indicates that the key factors inducing slagging should be high sodium and calcium contents, rather than melting and ferrum content.

Table 1. Typical properties of coal and ash used in this study

Samples	ZD coal	ZN coal
Proximate analysis		
Water content (wt%, ar)	26.4	13.1
Water content (wt%, ad)	14.78	9.19
Ash (wt%, ar)	5.44	12.94
Volatile matter (wt%, daf)	30.66	35.04
Fix carbon????????????	?????	?????
Lower heating value (MJ/kg, ar)	19.33	21.95
Ultimate analysis		
C_{ar}(wt%,ar)	54.38	58.71
H_{ar}(wt%,ar)	2.35	3.23
N_{ar}(wt%,ar)	0.47	0.68
O_{ar}(wt%,ar)	10.55	10.7
$S_{t,ar}$(wt%,ar)	0.41	0.64
Ash fusion temperatures		
DT(^{o}C)	1290	1170
ST(^{o}C)	1300	1180
HT(^{o}C)	1310	1190
FT(^{o}C)	1320	1330
Chemical components in ash		
SiO_2(wt%)	17.38	44.9
Al_2O_3(wt%)	7.68	17.33
Fe_2O_3(wt%)	8.02	9.01
CaO(wt%)	40.69	13.36
MgO(wt%)	6.6	5.04
Na_2O(wt%)	6.07	1.34
K_2O(wt%)	0.55	1.26
TiO_2(wt%)	0.65	0.71
SO_3(wt%)	11.32	6.47
MnO_2(wt%)	0.087	0.066

Note: ar-as received basis; ad-air dry basis; daf-dry and ash free; DT-deformation temperature; ST-softening temperature; HT-hemispherical temperature; FT-flowing temperature.

2.2 Slag and Deposit Sampling in a Full-Scale Boiler

Slags and deposits were sampled in a 350 MW tangential-fired boiler (Model, DG1211/17.4-II22) after continuous operating for six months. As shown in the Figure 2, five layers of burners (a, b, c, d, and e) were running, in which three

layers (b, c, and e) were used for ZD coal combustion and the other two layers (a, d) were for ZN coal. Because the coal feeding quantity in each layer is the same, the co-firing ratio of ZD coal is about 60 %, and the remaining 40 % if of ZN coal. The sampling positions are also marked in the Figure 2. They are located on each convection heating surface along the gas flow direction: wall reheater (A-WR), separation platen superheater (B-DPS), platen superheater (C-PS), medium and high temperature reheater (D-MHR), high temperature superheater (E-HS), low temperature superheater (F-LS), economizer (G-Eco), air preheater (H-Pre).

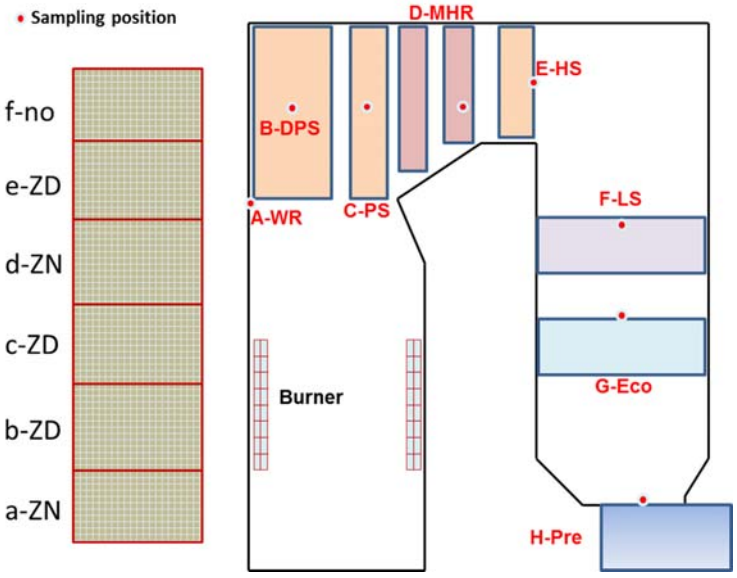

Figure 2. The slag and deposit sampling positions in a 350 MW pulverized coal furnace (ZD-Zhundong Coal, ZN-Zhunnan Coal).

2.3 Evaporating and Condensing of Ash Species

The evaporating and re-condensing test was operated in the schematic experimental system in Figure 3, mainly including evaporating unit and condensation sampling unit. The crucible containing biomass was heated in a tube furnace for ash evaporating. An S-type thermocouple was inserted from furnace bottom to measure the evaporating temperature. The temperature-controlled condensation sampling unit was 5 cm above the crucible, in order to capture the evaporated metal species for one hour. The sampling unit was cooled by air and the sampling substrate at the bottom was dismountable for further analysis. A K-type thermocouple was welded on the substrate inner surface to measure the condensing surface temperature, which was controlled at 500 ±5 ^{o}C by adjusting air speed. This condensing temperature range was used, since in the previous work by Schofield [17] it was reported that the deposition rate of sodium salts was almost unchanged with probe temperature changing, when the probe temperature is below 550 ^{o}C.

The fuel sample was heated from ambient temperature to three targeted temperatures: 500 °C, 800 °C, and 1000 °C at a constant heating rate of 5°C/min. The entire evaporating process was divided into three stages and the condensed metal vapor species were continuously sampled at each stage by changing a new substrate.

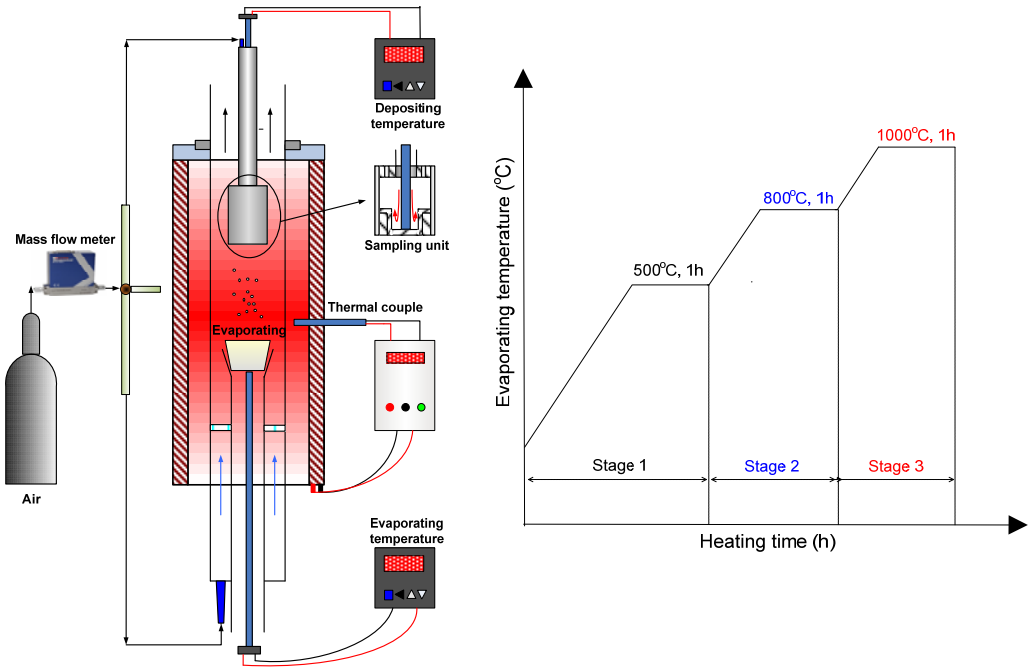

Figure 3. The experimental system for ash evaporating and depositing (left: experimental apparatus; right; heating process in this study)

The evaporation and condensation sampling were continuous in this apparatus, thus it was impossible to obtain the residual ash sample in the crucible for analysis. Therefore, the ash was again prepared in an atmosphere-controlled muffle furnace (KSL-1700X, made by Hefei Ke Jing Materials Technology Co., Ltd., China) by the heating curve shown in Figure 3, at 400, 600, 800, 1000, and 1100 °C under air atmosphere. The total flow rate passing through the furnace and samples was controlled at 500ml/min (O_2, 100ml/min; N_2, 400ml/min).

2.4 Characterization of Slag and Deposit Samples

X-ray fluorescence (XRF, S4 PIONEER, Germany) and X-ray diffraction (XRD, X'pert MPD Pro, PANalytical, Netherlands) were used to analyze the element distribution and the chemical components of the deposits from full-scale furnace, and of the residual ash from the muffle furnace. The micro-morphology and the element distribution in the condensed deposits on sampling substrate surfaces, were analyzed by using scanning electron microscopy–electron dispersive X-ray spectroscopy (SEM–EDX, JEOL JSM-6390A, Japan).

3. Results and Discussion

3.1 Morphology and Chemical Components of Deposit Samples in a Full-Scale Boiler

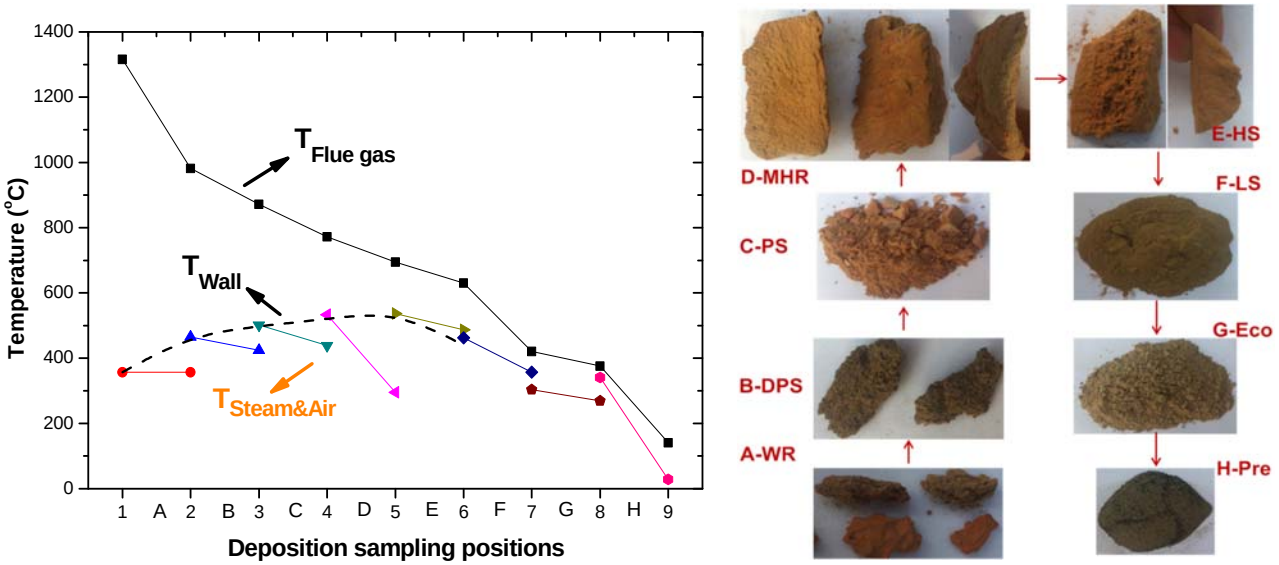

(a) *(b)*

Figure 4. The temperatures of (a) flue-gas/steam/wall and (b) the macro morphology of slags/deposits along sampling positions

The flue gas, steam, air, and wall temperature at each heating surface were collected, from power plant control system, and plotted in Figure 4(a). The morphologies of slags and ash deposits along gas flow direction are shown in Figure 4(b). It can be seen that all the slags and deposits from A-WR to E-HS have a dark-red color, which can bee associated to the presence of the ferrous oxides. In the region of high flue gas temperatures (A-WR and B-DPS, $T_{flue\ gas}$>872 ºC), there are a certain amount of dark porous slags. In medium gas temperature regions (C-PS, D-MHR, and E-HS, 872 ºC >$T_{flue\ gas}$>630 ºC), there was no dark porous slags and these compacted deposits looked like blocky red soil. At last three heating surfaces (F-LS, G-Eco, and H-Pre, 630 ºC >$T_{flue\ gas}$>141 ºC), no blocky deposit was found, and there was mainly the loose ash stacking on horizontal tube surfaces. The samples in Figure 4 can be divided into three groups: dark porous slags, compacted dark-red blocks, and loose ash stackings.

The elemental compositions for all the deposit samples collected on each surfaces are displayed as stacked columns in Figure 5(a). It can be seen that the top three elements in most deposits are silicon, calcium, and sulfur, corresponding to the co-firing ratio, ash and inorganic elemental content in raw fuels. The ash content in ZN coal is more than twice of that in ZD coal, and silicon content in ZN coal ash is almost 45% while that in ZD coal is below 18%. The calcium

content ranks the first (~40%) and third (~13%) in ZD and ZN coal ash, respectively. The sulfur contents in these deposits range from 11% to 24%, much higher than the ash sulfur contents in Table 1. This indicates that sulfur oxides released from volatile and char react with inorganic ash species, and form sulfates that deposit on the ash or heating surfaces. The sodium content is comparably low and stable ranging from 3 to 5%.

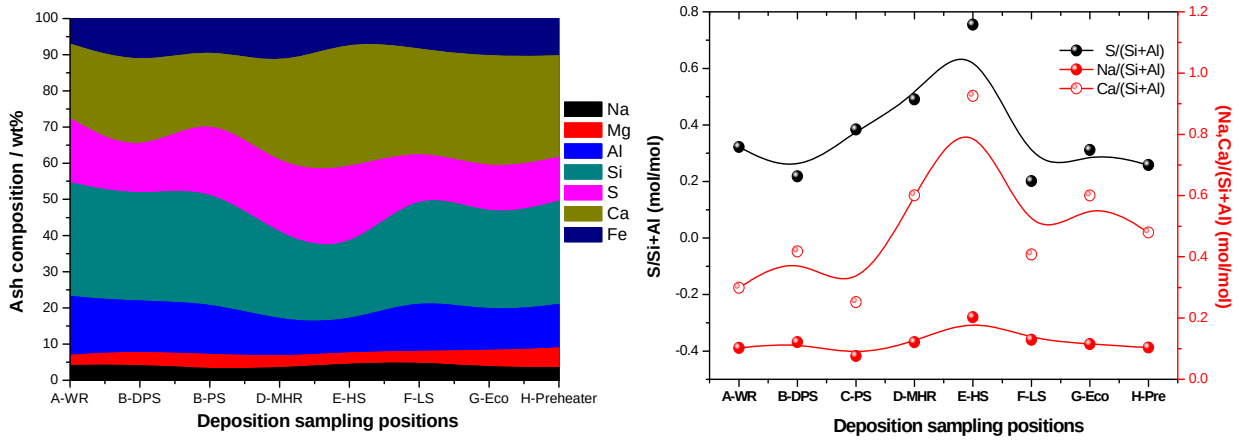

(a) *(b)*

Figure 5. Elemental composition (a) and ratios of S/Na/Ca:Si+Al (b) in the deposit along heating surfaces.

In Figure 5(a), it can also be observed that in the region of D-MHR and E-HS, the contents of calcium and sulfur were suddenly enlarged while the contents of silicon and aluminum were lowered. This indicates that calcium and sulfur species have higher concentrations in these two regions. To show it more clearly, the mass ratios of S/(Si+Al), Ca/(Si+Al), and Na/(Si+Al) are shown in Figure 5(b). In Figure 5(b), the significant increase of sulfur, calcium, and sodium content in D-MHR and E-HS regions can be observed. These three element contents in E-HS region are 2.5 times than that in A-WR, B-DPS, F-LS, G-Eco, and H-Pre regions.

Comparing the flue gas temperature in Figure 4(a) with the elemental composition in Figure 5(b), it can be seen that from A-WR to C-PS, the flue gas temperature decreases from 1316 to 872 °C, and there is no apparent increase of sodium, calcium, and sulfur content. However, from C-PS to D-MHR, with the flue gas temperature further decreases from 872 to 772 °C, a sharp increase in sodium, calcium, and sulfur content can be observed. This proves that in the temperature range of 872 to 772 °C, amount of gaseous sodium and calcium sulfates condense into sulfate aerosols and then deposit on ash particle and heating surfaces. The condensing and depositing quantity of sulfates reaches the highest value at 695 °C, in E-HS region. Most sulfates condense and deposit in D-MHR and E-HS region (872 °C to 630 °C),

since at the last three heating surfaces (F-LS, G-Eco, and H-Pre, 630 ^{o}C >$T_{flue\ gas}$>141 ^{o}C), sulfate content in deposits and ash is almost constant.

The observed phenomenon is very similar with our previous studies related to the ash deposition in a full-scale grate furnace burning biomass with high potassium content [18]. In biomass furnaces, the gaseous sodium sulfates in flue gas also started its condensing and depositing on medium heating surfaces below 900 ^{o}C. This indicated that, when combusting fuels with high contents of AAEMs, there is a critical temperature around 850 ^{o}C, at which most of the AAEMs sulfates start to condense, form aerosols, and to deposit.

Table 2. The qualitative chemical components by XRD (color depth standing for content)

Position / Component	A	B	C	D	E	F	G	H
$CaSO_4$, Calcium sulfate								
Fe_2O_3, Hematite								
SiO_2, Quartz								
$NaAlSiO_4$, Nepheline								
$(Na,Ca)(Si,Al)_4O_8$, Albite								
NaS Na_2S, Sodium sulfide								
$Al_2Ca_3Si_2$, Aluminium calcium silicon								
$Al_6Si_2O_{13}$, Mullite								

XRD analysis was conducted to qualitatively identify the major and minor mineral components in slags and deposits shown in Table 2. In this table the pane color depth stands for mineral content level. The eight samples were divided into two groups: in the first group (A-E) $CaSO_4$ ranked the first, while in the second group (F-H) SiO_2 ranked the first. This is corresponding to the macro morphology and elemental composition results. The samples in first group are mainly porous slags and blocky deposits, due to the melting at high temperatures and condensing at medium temperatures. In the second group, since already most of sulfates have condensed and deposited in previous regions, $CaSO_4$ content in this group of deposits decreases, SiO_2 and $Al_6Si_2O_{13}$ contents increase. Therefore these samples look like loose ash containing more aluminosilicates. Moreover, the authors tried to find sodium sulfates in the samples,

however, no Na_2SO_4 was found, only some minor minerals like $NaAlSiO_4$, $(Na,Ca)(Si,Al)_4O_8$, and Na_2S. The named minerals were also mainly detected in the regions of C-PS, D-MHR, and E-HS, at medium gas temperatures.

3.2 Chemical Component of Coal Ash at Different Evaporating Temperatures

The full-scale co-firing test gives the chemical components of slags and deposits on heating surfaces in boilers, which clearly showed the enrichment and depositing of calcium sulfates on heating surfaces. However, due to the co-firing of ZD and ZN coal, and relative lower content of sodium, 1/8 of calcium content, the enrichment of sodium species in deposits was not observed. To further demonstrate the evolution of sodium from the raw Zhungdong coal to deposits, the experiments of ash evaporating and re-condensing were conducted.

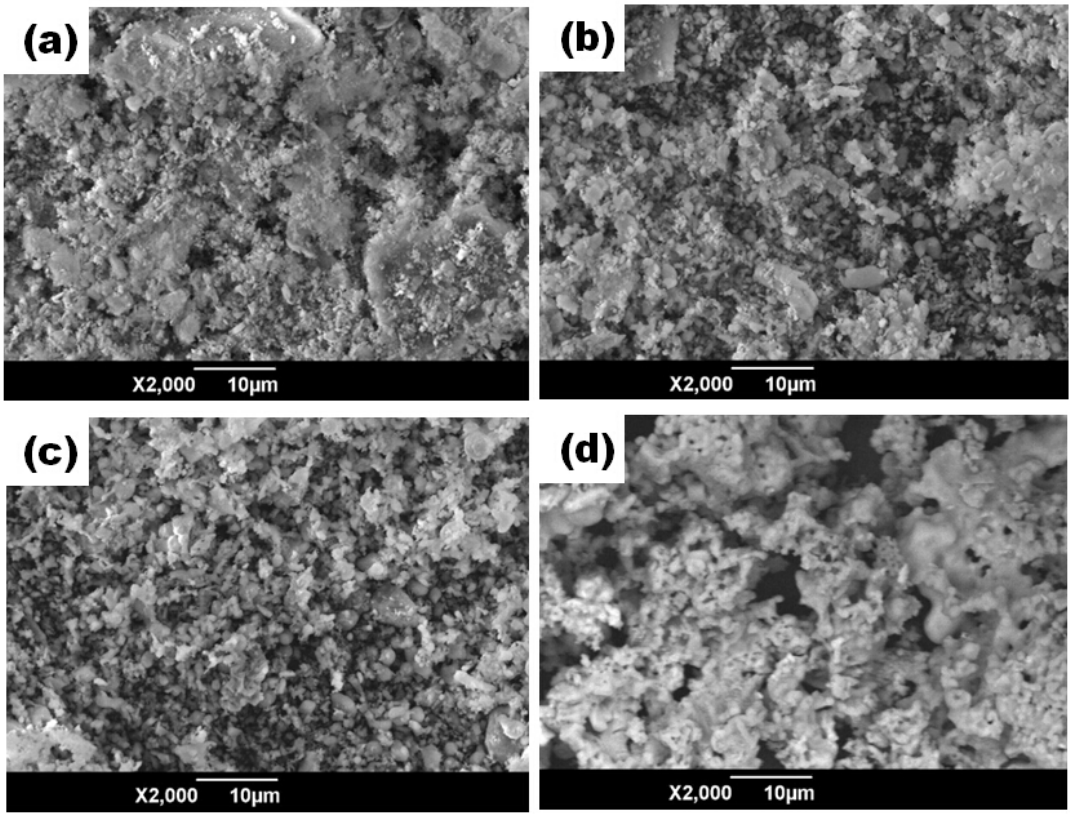

Figure 6. Residual ash morphologies at (a)-600°C, (b)-815°C, (c)-1000°C, (a)-1100°C

Zhundong coal ash was mainly prepared in a muffle furnace at temperatures ranging from 400 to 1400 °C in air atmosphere. At the temperatures of1200 °C and 1400 °C, the ash samples melted, flowed, adhered to the alundum plate, and were impossible to be analyzed. The SEM micro morphologies of ash prepared at 600, 815, 1000, and 1100 °C are shown in Figure 6. With the temperature increasing from 600 to 1000 °C, the ash particles size decreased with no

conspicuous sintering. However, when the temperature was continually increased to 1100 ºC, significant sintering occurred, ash particles melted, and aggregated into large porous pieces. In this study, the heating time in muffle furnace is one hour at targeting temperatures, while the practical residence time of coal and ash particles in boilers is only 3-6 s, which seems incomparable. However, those ash particles depositing and adhering on heating surfaces indeed undergo a much longer period. With the increasing in deposits thickness on heating surfaces, the heating transfer efficiency is significantly reduced, and the wall or deposits temperature can increase from 500 to 1200 ºC [13]. At such a high local wall temperature (>1100 ºC), ash particles on wall surfaces melt, aggregated, and tightly adhered on unclean heating surfaces.

The elemental composition of ash at different temperatures is shown in Figure 7(a). With the increasing in ashing temperature, sodium and potassium content decrease, and at temperature of 1000 ºC, there is almost no alkali metal. In contrast, for the elements like silicon and aluminum, their contents in ash increase with temperature increasing. The change of oxygen content is also draws attention. Due to its decreasing with temperature, this phenomena indicates partial minerals release as oxides. Moreover, what should be noted is that sulfur content decreases at 1000 ºC and becomes zero at 1100 ºC.

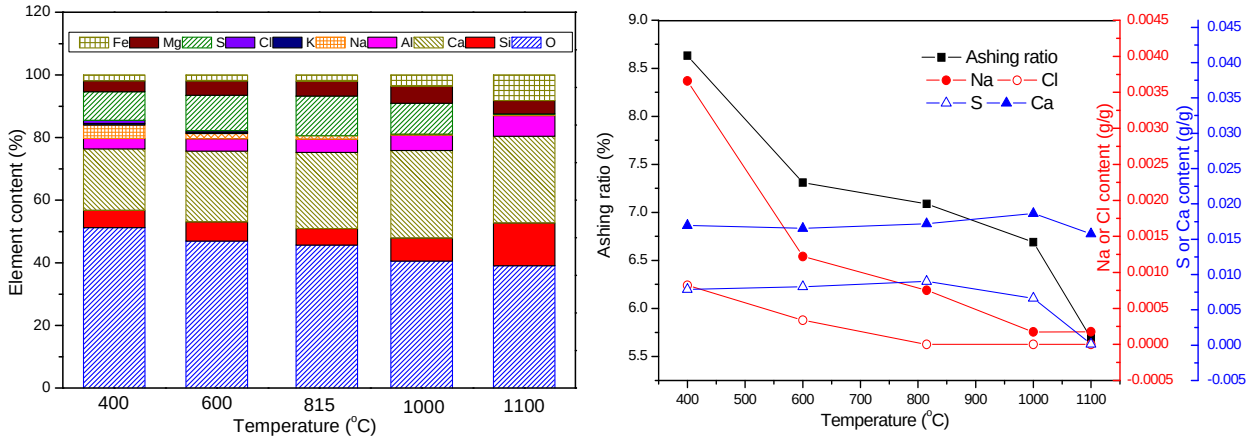

(a) *(b)*

Figure 7.The elemental composition (a) and the residual key element mass (Na/Cl/S/Ca) per gram coal (b) at different ashing temperatures

Multiplying the elemental content (%) with ashing ratio (%), and raw sample mass (g), to reveal the elemental evaporating more clearly, the absolute residual mass of key elements per gram ZD coal can be calculated. These values are plotted in Figure 7(b). The right Y axis scale of calcium and sulfur is 10 times of that of sodium and chlorine to keep them in one figure comparably. With the increasing in ashing temperature from 400to 1200 ºC, the evaporating process

can be divided into three stages identified by the curves of ashing ratio and residual element mass. The first stage, from 400 to 815 °C, 80 % of sodium, and 100 % of chlorine were released. The second stage, from 800 to 1000 °C, all the left sodium evaporated and sulfur started to be released. The third stage, from 1000 to 1100 °C, all the left sulfur was released and calcium started its evaporating.

The release of chlorine in Zhundong coal was very similar with our previous investigation for biomass fuel, in which all chlorine was also released at around 800 °C [19]. A previous XAFS study showed that all the chlorine in brown coal was likely to be associated with sodium [3]. Here it can be noted that in Figure 7(b) the released mass quantity of chlorine was much less than that of sodium, which indicated that only partial sodium was released as chloride and the other might be released as atom, oxide, and hydroxide. The calcium in coal ash was very stable and released only when the temperature was higher than 1100 °C. Most of alkaline earth metals (Ca and Mg) existed as ion-exchangeable carboxylates in raw coal, which decomposed and produced oxides at low temperatures (< 900 °C) [20]. However, when the temperature increased, partial calcium oxide evaporated, reacting with silicon and aluminium oxides.

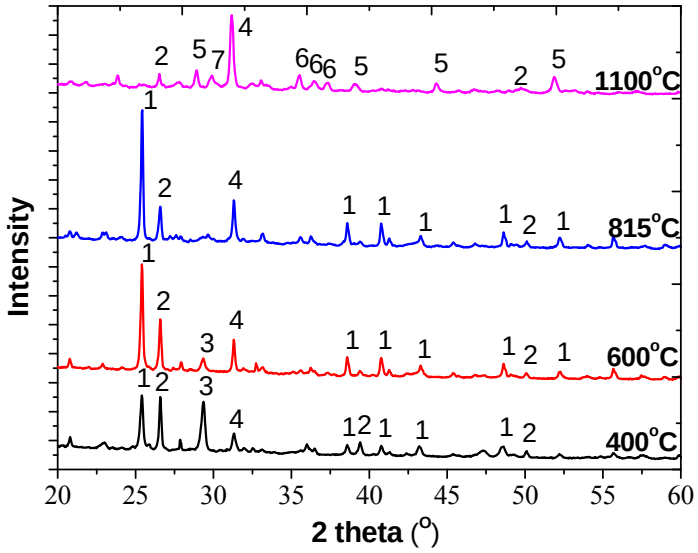

Figure 8.XRD patterns of ash prepared at different ashing temperatures (1- anhydrite,$CaSO_4$; 2- quartz,SiO_2; 3- calcium carbonate, $CaCO_3$; 4- gehlenite, $Ca_2Al_2SiO_7$; 5- akermanite,$CaMgSi_2O_7$; 6- wollastonite,$CaSiO_3$; 7- augite,$Ca(Mg,Fe)Si_2O_6$

XRD patterns were measured to further illustrate the transformation of minerals, and are shown in Figure 8. The Figure 8 shows that in the original ash at 400 °C, the major minerals include anhydrite ($CaSO_4$), quartz (SiO_2) and calcium carbonate ($CaCO_3$) with a very strong signal peak, respectively. There is also a small amount of gehlenite ($Ca_2Al_2SiO_7$)

at this temperature. As the heating temperature increased to 600 °C, the XRD peak intensity of $CaCO_3$ greatly decreased, referring to the decomposition of $CaCO_3$:

$$CaCO_3 \longrightarrow CaO+CO_2(g) \quad \text{(R1)}.$$

It was also found that at 600 °C, the XRD peak intensity of SiO_2 decreased but that of $Ca_2Al_2SiO_7$ increased, which indicated partial silicon oxides and aluminum oxides might react with calcium oxides to generate gehlenite at a lower temperature through:

$$2CaO+SiO_2+Al_2O_3 \longrightarrow Ca_2Al_2SiO_7 \quad \text{(R2)}.$$

When the heating temperature was increased the heating temperature to 815 °C, it was observed that $CaCO_3$ disappeared, SiO_2 content further decreased, while the peak intensity of $Ca_2Al_2SiO_7$ exceeded that of SiO_2. This even more affirmed the possibilities of reactions R1 and R2 indicated above. Besides of the reaction R2 from CaO to $Ca_2Al_2SiO_7$, $CaSO_4$ was also proposed to react with SiO_2 and Al_2O_3 to produce $Ca_2Al_2SiO_7$ at around 800 °C [21].

When the ash was prepared at 1100 °C, the XRD patterns have been totally changed. In the temperature ranging from 400 °C to 815 °C, $CaSO_4$ and SiO_2 were always the most abundant mineral species in ash, while at the temperature of 1100 °C these two mineral species almost totally decomposed. At 1100 °C the XRD peak intensity of $Ca_2Al_2SiO_7$ increased again, proving that more gehlenites were formed at higher temperatures by reaction R2. Moreover, it can be noted that at the temperature of 1100 °C $CaMgSi_2O_7$ and $CaSiO_3$ were formed, indicating that with the decomposing of $CaSO_4$, CaO reacted with SiO_2 to form wollastonite ($CaSiO_3$). Akermanites ($CaMgSi_2O_7$) and augites ($Ca(Mg,Fe)Si_2O_6$) were also found with the participation of magnesium oxides and ferrum oxides. Our previous results have proved that SiO_2 is highly efficient to promote the decomposition of $CaSO_4$. Consequently, the evolution mechanism of Zhundong coal ash with high calcium and sulfur content at higher temperature than 1000°C can be concluded as following:

$$CaSO_4 \longrightarrow CaO+SO_3(g) \quad \text{(R3)}$$

$$CaO+SiO_2 \longrightarrow CaSiO_3 \quad \text{(R4)}$$

$$CaSO_4+SiO_2 \longrightarrow CaSiO_3+SO_3(g) \quad \text{(R5)}$$

$$CaO+MgO+ xSiO_2 \longrightarrow CaMgSi_2O_7 \quad \text{(R6)}$$

$$CaO+MgO+Fe_yO_z+SiO_2 \longrightarrow Ca(Mg,Fe)Si_2O_6 \quad \text{(R7)}.$$

3.3 Micro-morphology and Elemental Component of Re-condensing Deposits after Evaporating

In the previous section, the residual ash properties at different evaporating temperatures have been declared clearly. However, the evolution of sodium was still not clearly demonstrated by XRD, due to its lower content, compared to other major mineral elements in ash. In this study, a moderate quench method was used to obtain re-condensed sodium species at the wall temperature of 500 ºC. Since the distance from the evaporating unit to the quench probe bottom is short, the condensed and deposited species on the probe bottom, are capable to represent the forms of released inorganic elements from ZD coal combustion.

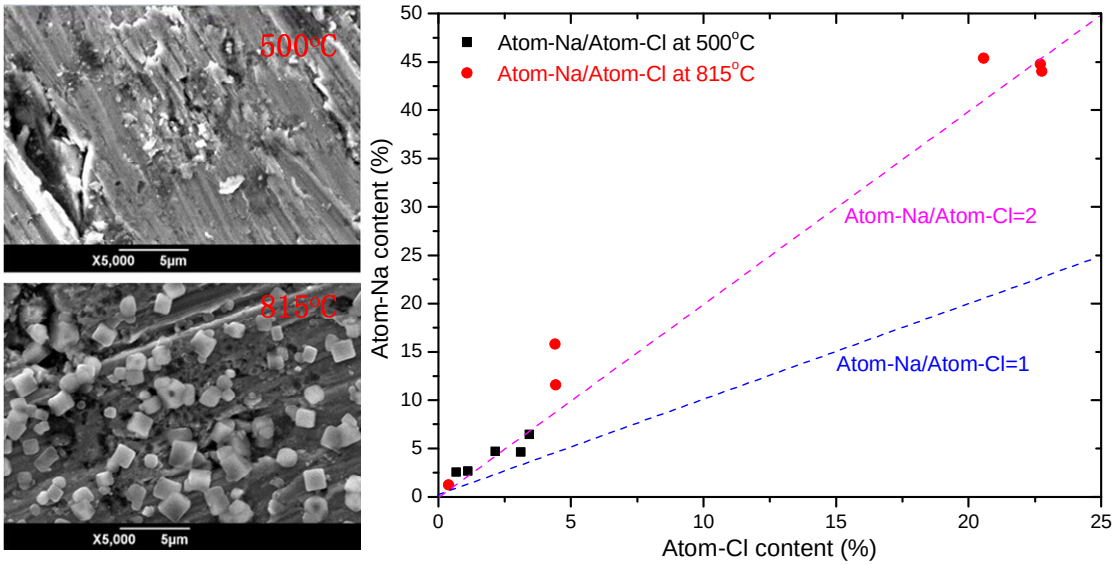

Figure 9. The micro structures and Na/Cl contents in the condensing deposits at lower evaporating temperatures (evaporating temperature = 500 ºC and 815 ºC).

The micro-morphology of re-condensed species from biomass combustion at 500 and 815ºC is shown in Figure 9 (left). When biomass was burned at 500 ºC, there was no remarkable crystal deposition on the probe bottom, while at 815 ºCcubic shaped crystal particles were observed. The element contents of deposits on probe bottom was analyzed by using EDS for more than ten target points. It was found that there were mainly sodium and chlorine in the deposits, besides of the basic elements of ferrum and chromium for all the tested points. The atom mole contents of sodium and chlorine in crystals was collected and is plotted in the Figure 9 (right). The Figure 9 (right) shows that most of points deviate from the line of Na:Cl=1:1, but are adjacent to the line of Na:Cl=2:1, or are in the area of Na:Cl>2:1. This indicated that only 50% or less of sodium was released in the form of NaCl, and the other sodium might be released in the form of atoms. Eyk et al. [5] investigated sodium release from Loy Yang brown coal by using quantitative planar laser-induced fluorescence measurement and equilibrium calculation. The study showed that besides of sodium chlorides,

the most likely sodium compound in ash is sodium oxide. This leaded to the release of atomic sodium from ash at high temperatures. However, sodium was hardly to be released into the flue gas in the form of Na_2O or NaOH, because even if NaOH was produced by Na_2O and H_2O at high temperatures, it would also equilibrate to produce atomic Na [22]. The results of chemical equilibrium calculation for sodium compounds by Takuwa and Naruse [23] also indicated that there was no gaseous NaOH at the temperature below 1100 °C. However, another work on particulate matter emission from brown coal combustion found NaCl mainly contributed to the emission of particles with aerodynamic diameter less than 0.1μm [24]. Li [3] reviewed the existing forms of sodium in Victorian brown coal with high content of AAEMs, which is very similar to Zhundong coal. In this brown coal, sodium species can mainly be found in two forms: as ion-exchangeable cations associated with the carboxyl groups forming part of organic coal substance or as NaCl associated with the moisture in coal [3-4, 25]. Consequently, in this study, the cubic crystal of NaCl on probe surfaces should be from the NaCl combined with the moisture in Zhundong coal, and the other atom sodium should be from the sodium associated with the carboyl groups in Zhundong coal.

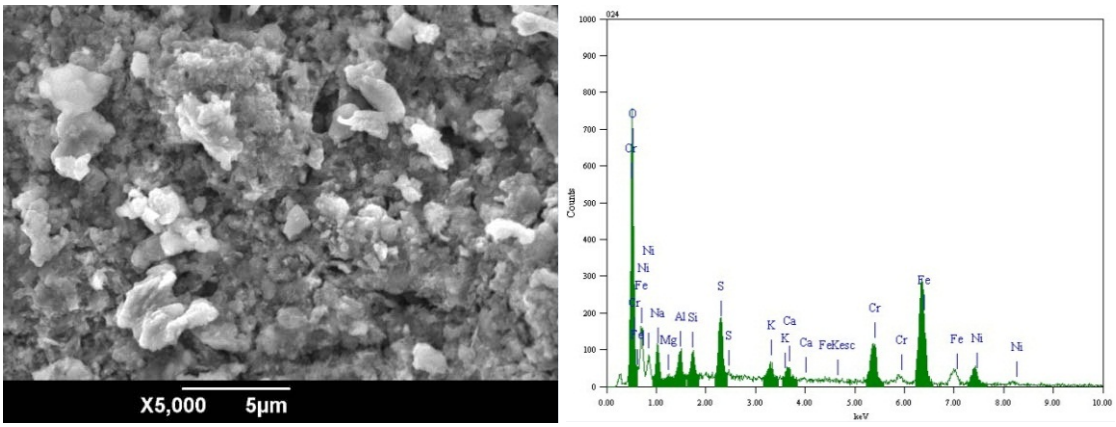

(a) Global micro structures and element contents

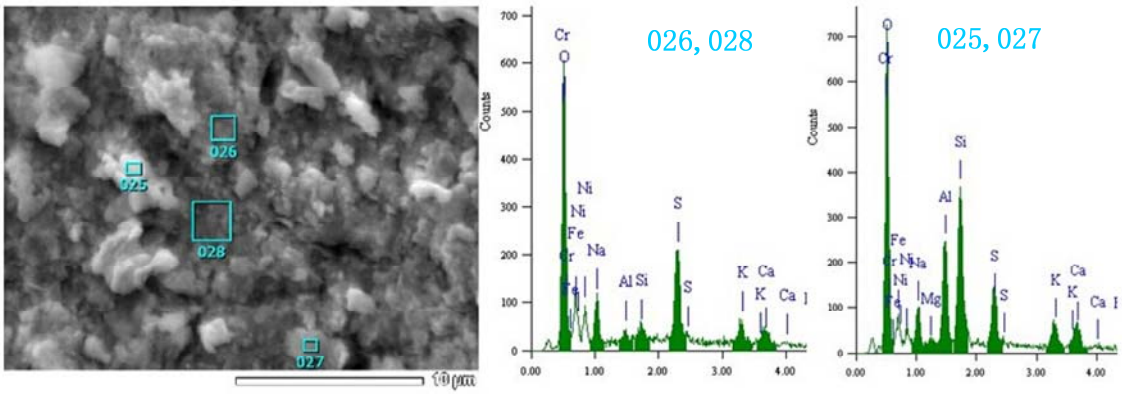

(b) Comparison of different types of deposits

Figure 10. The micro stuctures and elment contents in the deposits at a higher evaporating temperature (evaporating temperature = 1000°C).

After the ash was heated to 815 °C, the third clean deposition probe, also cooled and with the surface temperature of 500 °C, was inserted, and the heating temperature was increased to 1000 °C and kept constant for one hour. The global micro structures and element contents in deposits are shown in Figure 10 (a). It can be seen that there was no chlorine in the deposits, agreeing well with the results in Figure 9 (b), since all the chlorine has been released before the temperature of 815 °C. Whereas, as shown in Figure 10 (a), sulfate species were observed in the deposits at evaporating temperature of 1000°C. Also in this figure a small amount of silicon and aluminum can be observed, indicating the depositing of aluminosilicates. Furthermore, a selected measurement on the element distribution of different kinds of deposits is shown in Figure 10 (b). At evaporating temperature of 1000 °C, the deposits on the probe were mainly divided into two types: (1) the sulfates of alkali and alkaline earth metals (SAAEMs) containing sulfur, sodium, potassium, and calcium; (2) the aluminosilicates containing silicon, aluminum, sodium, potassium, calcium, and magnesium. As shown in Figure 10 (b), the first type was grey and noted as 026 and 028, while the second type was light white and noted as 025 and 027. Most of the light white particles were embedded into the grey layer at the bottom. This proved that in the ash depositing process of Zhundong coal combustion, the released or formed gaseous sodium chlorides, sodium sulfates, calcium sulfates, and potassium sulfates firstly deposited on the cooling surfaces, and then partial aluminosilicates were captured and embedded into the first layers.

3.4 Temperature-Dependent Ash Deposition Mechanism in Zhundong Coal Combustion

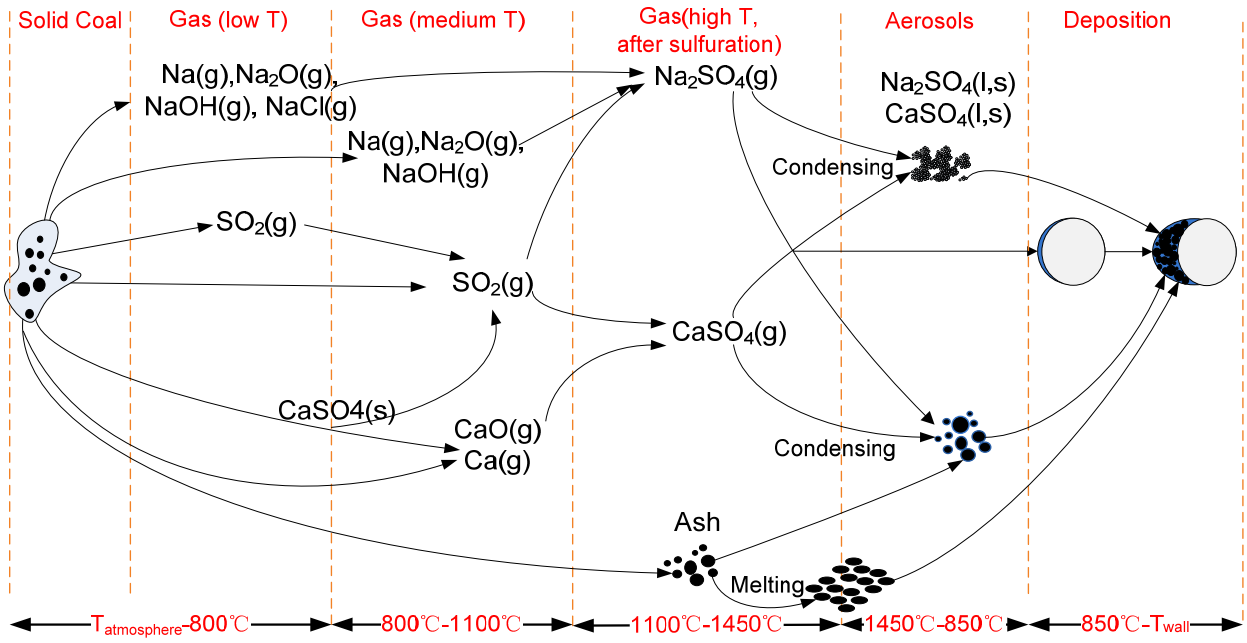

Figure 11. The possible ash depositing mechanism in the combustion of Zhundong coal with high sodium and calcium contents.

Based on the results from the full-scale industry boiler and lab-scale experiments, a temperature-dependent ash deposition mechanism cor the combustion of Zhundong coal, with high sodium and calcium content, in pulverized coal furnaces was proposed in Figure 11. At a lower temperature of 800 °C, more than 80% of the sodium in Zhundong coal was released into flue gas in the form of atom sodium, sodium oxides, hydroxide, and chlorides; SO_2 was mainly from the oxidation of organic sulfur and pyrites. With the temperature increased to 1100 °C, the left sodium was mainly released in non-chloride form, while all the left sulfur in calcium sulfates was released by the decomposition of calcium sulfates with the formation of calcium oxides. Starting from 1000 °C, partial calcium has been released as gaseous forms of calcium oxides and atom calcium. As the temperature increased, as high as the flame temperature in pulverized coal furnace, all the sodium and most of the calcium should be released as gaseous species, which quickly reacted with sulfur oxides in the flue gas, forming a large amount of gaseous calcium and sodium sulfates [26-27]. At the temperature ranging from 1100 to 1450 °C, Zhundong coal ash melts and was easy to be adhered on cooling surfaces.

After the flue gas passes through the convection heating surface, its temperature is reduced. With the decreasing in flue gas temperature, the aerosols of calcium and sodium sulfates started forming. When the flue gas temperature decreased to around 850 °C, a large number of sulfate aerosols are formed, which very easily deposit on heating surfaces. These aerosols could also deposit on the surfaces of fly ash, aggravating the adhering of ash particles on heating surfaces.

In the meantime, the gaseous sulfates around the cooling surfaces directly condense and deposit on the surfaces. The depositing of sulfate aerosols and condensed sulfates on heating surfaces is especially important, since after the formation of such a layer, more and more fly ash particles were adhered and the depositing layer would grow up quickly.

4. Conclusions

In this work, the Ca/Na/S/Cl transformation and ash deposition mechanism in boilers burning Zhundong coal with high calcium and sodium contents was demonstrated. The main conclusions are as following:

(1) In a full-scale boiler, the condensing and depositing of sodium and calcium sulfates play an important role on the slagging and ash depositing on convection heating surfaces. Sulfates start to significantly condense and deposit at the flue gas temperature of about 850 ^{o}C (at Medium and High Temperature Reheater).

(2) With the increasing in temperature from 400 to 1200 ^{o}C, the ash evaporating process is divided into three stages: a) from 400 to 800 ^{o}C, 80% of sodium, and 100% of chlorine are released; b) from 800 to 1000 ^{o}C, all the left sodium evaporated and sulfur starts to be released with the formation of partial aluminosilicates; c) from 1000 to 1200 ^{o}C, all the left sulfur is released through the decomposition of calcium sulfates and then calcium starts to evaporate, while silicon oxides disappears due to the formation of new complex silicates.

(3) The condensing quenching test further proved the detailed forms of released sodium and calcium. The sodium in Zhundong coal was released mainly in the forms of atom, oxide, hydroxide, and chloride, in which sodium chloride account for less than 50 %. When the evaporating temperature increased higher than 1000 ^{o}C, partial alkali and alkaline earth metals were released as gaseous sulfates, and afterwards condense and deposit on the heating surfaces.

Acknowledgment

This study was supported by the National Natural Science Foundation of China (Nos. 51376147 and 51306142).

References:

[1] J. Xu, D. Yu, B. Fan, X. Zeng, W. Lv, J. Chen, Characterization of Ash Particles from Co-combustion with a Zhundong Coal for Understanding Ash Deposition Behavior, Energy & Fuels, 28 (2013) 678-684.

[2] J. Li, X. Zhuang, X. Querol, O. Font, N. Moreno, J. Zhou, Environmental geochemistry of the feed coals and their combustion by-products from two coal-fired power plants in Xinjiang Province, Northwest China, Fuel, 95 (2012) 446-456.

[3] C.-Z. Li, Some recent advances in the understanding of the pyrolysis and gasification behaviour of Victorian brown coal, Fuel, 86 (2007) 1664-1683.

[4] H. Wu, D.M. Quyn, C.-Z. Li, Volatilisation and catalytic effects of alkali and alkaline earth metallic species during the pyrolysis and gasification of Victorian brown coal. Part III. The importance of the interactions between volatiles and char at high temperature, Fuel, 81 (2002) 1033-1039.

[5] P.J. van Eyk, P.J. Ashman, Z.T. Alwahabi, G.J. Nathan, The release of water-bound and organic sodium from Loy Yang coal during the combustion of single particles in a flat flame, Combustion and Flame, 158 (2011) 1181-1192.

[6] P.J. van Eyk, P.J. Ashman, Z.T. Alwahabi, G.J. Nathan, Simultaneous measurements of the release of atomic sodium, particle diameter and particle temperature for a single burning coal particle, Proceedings of the Combustion Institute, 32 (2009) 2099-2106.

[7] Z. Yang, J. Liui, W. Yao, Fouling index of Zhundong coal ash, Clean Coal Technology, (2013) 81-84.

[8] J. Chang, Z. Yang, Study on Zhundong Coal's Ash Fouling Indicator to Ensure Safe Operation of Boilers, Boiler Technology, (2013) 17-19.

[9] B.-Q. Dai, F. Low, A. De Girolamo, X. Wu, L. Zhang, Characteristics of Ash Deposits in a Pulverized Lignite Coal-Fired Boiler and the Mass Flow of Major Ash-Forming Inorganic Elements, Energy & Fuels, 27 (2013) 6198-6211.

[10] L. Harbin Boiler Co., Investigation on the combustion characteristics of Zhundong coal and the feasibility study on the design of furnace fully burning Zhundong coal, in, 2012.

[11] Y. He, J. Zhu, B. Li, Z. Wang, Z. Li, M. Aldén, K. Cen, In-situ Measurement of Sodium and Potassium Release during Oxy-Fuel Combustion of Lignite using Laser-Induced Breakdown Spectroscopy: Effects of O2 and CO2 Concentration, Energy & Fuels, 27 (2013) 1123-1130.

[12] H. Zhou, B. Zhou, H. Zhang, L. Li, K. Cen, Investigation of Slagging Characteristics in a 300 kW Test Furnace: Effect of Deposition Surface Temperature, Industrial & Engineering Chemistry Research, 53 (2014) 7233-7246.

[13] H. Zhou, B. Zhou, L. Li, H. Zhang, Experimental Measurement of the Effective Thermal Conductivity of Ash Deposit for High Sodium Coal (Zhun Dong Coal) in a 300 KW Test Furnace, Energy & Fuels, 27 (2013) 7008-7022.

[14] J. Meng, Research on Combustion and Slagging Characteristics of Zhundong Coal, in, Harbin Institute of Technology, 2013.

[15] Y. Wang, Q. Zhao, H. Ma, H. Wang, W. Jiang, Experimental Study on Ash Fusion Characteristics of Zhundong Coal, Journal of Chinese Society of Power Engineering, 33 (2013) 841-846.

[16] J. Fan, Research on Zhundong Coal's Slagging Characteristics and Its Ash Fusibility of Blending Coal, in, Zhejiang University, 2014.

[17] K. Schofield, The chemical nature of combustion deposition and corrosion: The case of alkali chlorides, Combustion and Flame, 159 (2012) 1987-1996.

[18] M.U. Garba, D.B. Ingham, L. Ma, R.T.J. Porter, M. Pourkashnian, H.Z. Tan, A. Williams, Prediction of Potassium Chloride Sulfation and Its Effect on Deposition in Biomass-Fired Boilers, Energy & Fuels, 26 (2012) 6501-6508.

[19] X. Wang, J. Si, H. Tan, L. Ma, M. Pourkashanian, T. Xu, Nitrogen, Sulfur, and Chlorine Transformations during the Pyrolysis of Straw, Energy & Fuels, 24 (2010) 5215-5221.

[20] X. Gao, M.U. Rahim, X. Chen, H. Wu, Significant contribution of organically-bound Mg, Ca, and Fe to inorganic PM10 emission during the combustion of pulverized Victorian brown coal, Fuel, 117, Part A (2014) 825-832.

[21] X. Wei, J. Huang, T. Liu, Y. Fang, Y. Wang, Transformation of Alkali Metals during Pyrolysis and Gasification of a Lignite, Energy & Fuels, 22 (2008) 1840-1844.

[22] T. Takuwa, I. Naruse, Emission control of sodium compounds and their formation mechanisms during coal combustion, Proceedings of the Combustion Institute, 31 (2007) 2863-2870.

[23] T. Takuwa, I. Naruse, Detailed kinetic and control of alkali metal compounds during coal combustion, Fuel Processing Technology, 88 (2007) 1029-1034.

[24] X. Gao, H. Wu, Combustion of Volatiles Produced in Situ from the Fast Pyrolysis of Woody Biomass: Direct Evidence on Its Substantial Contribution to Submicrometer Particle (PM1) Emission, Energy & Fuels, 25 (2011) 4172-4181.

[25] A.D. Shah, G.P. Huffman, F.E. Huggins, N. Shah, J.J. Helble, Behavior of carboxyl-bound potassium during combustion of an ion-exchanged lignite, Fuel Processing Technology, 44 (1995) 105-120.

[26] P. Glarborg, P. Marshall, Mechanism and modeling of the formation of gaseous alkali sulfates, Combustion and Flame, 141 (2005) 22-39.

[27] G.P. Huffman, F.E. Huggins, N. Shah, A. Shah, Behavior of basic elements during coal combustion, Progress in Energy and Combustion Science, 16 (1990) 243-251.

Table Captions

Table 1 Typical properties of coal and ash used in this study

Table 2 The qualitative chemical components by XRD (color depth standing for content)

Figure Captions

Fig. 1 The contents of Na, Ca and S in Xinjiang Zhundong Coal ash and Non-Zhundong Coal ash (eight kinds of Zhundong Coal and twenty-seven kinds of Non-Zhundong Coal, and e.g., 100/Na refering to the inverse of Na content in ash)

Fig. 2 The slag and deposit sampling positions in a 350 MW pulverized coal furnace

(ZD-Zhundong Coal, ZN-Zhunnan Coal).

Fig. 3 The experimental system for ash evaporating and depositing (left: experimental apparatus; right; heating process in this study)

Fig. 4 The temperatures of (a) flue-gas/steam/wall and (b) the macro morphology of slags/deposits along sampling positions

Fig. 5 Elemental composition (a) and ratios of S/Na/Ca:Si+Al (b) in the deposit along heating surfaces.

Fig. 6 Residual ash morphologies at (a)-600^{o}C, (b)-815^{o}C, (c)-1000^{o}C, (a)-1100^{o}C

Fig. 7 The elemental composition (a) and the residual key element mass (Na/Cl/S/Ca) per gram coal (b) at different ashing temperatures

Fig. 8 XRD patterns of ash prepared at different ashing temperatures (1- anhydrite,$CaSO_4$; 2-quartz,SiO_2; 3- calcium carbonate, $CaCO_3$; 4- gehlenite, $Ca_2Al_2SiO_7$; 5- akermanite,$CaMgSi_2O_7$; 6-wollastonite,$CaSiO_3$; 7- augite,$Ca(Mg,Fe)Si_2O_6$

Fig. 9 The micro structures and Na/Cl contents in the condensing deposits at lower evaporating temperatures (evaporating temperature = 500 ^{o}C and 815 ^{o}C).

Fig. 10 The micro stuctures and elment contents in the deposits at a higher evaporating temperature (evaporating temperature = 1000^{o}C).

Fig. 11 The possible ash depositing mechanism in the combustion of Zhundong coal with high sodium and calcium contents.